ORIENTAL JOURNAL OF CHEMISTRY
An International Open Access, Peer Reviewed Research Journal
www.orientjchem.org
ISSN: 0970-020 X
CODEN: OJCHEG
2024, Vol. 40, No.(5):
Pg. 1426-1439

Maxdo and RDF55v are Crucial Molecular Descriptors Governing the Cannabinoid Receptor 1(CB1) Modulator Activity of N, N'-diphenyl Urea Analogs and 1H-Indole-2-carboxamides

SHABIR H. LONE[1]*, SHAHEEN BEGUM[2] and WAHEED AHMAD KHANDAY[3]

[1]Department of Chemistry, Government Degree College Pampore, Tulbagh, 192121, Pulwama, J & K, India.
[2]Institute of Pharmaceutical Technology, Sri Padmavati Mahila Visvavidyalayam (Women's University), Tirupati 517502, Andhra Pradesh, India.
[3]PG Department of Chemistry Sri Pratap College Srinagar, Jammu & Kashmir-190001, India.
*Corresponding author E-mail: shaheen.pharmchem@gmail.com

http://dx.doi.org/10.13005/ojc/400526

(Received: July 08, 2024; Accepted: September 07, 2024)

ABSTRACT

CB1 allosteric modulators such as synthetic cannabinoids are promising therapeutic agents. Among the various CB1 receptor modulators, indole-2-carboxamides, and N, N'-diphenyl urea derivatives are continuously explored for their potency and selectivity towards the receptor. In the present computational work, QSAR models were generated using Drug Theoretics and Chemoinformatics (DTC tools) tools to analyze the influence of molecular features of these modulators (one hundred and fourteen compounds) on the activity. A statistically significant three-parameter model (SPMin2_Bhm, maxdO, and minssN) was derived that displayed R2 and Q2 values of 0.66 and 0.62, respectively. SPMin2_Bhm and maxdO negatively correlated with the activity, whereas minssN has a positive connection. A seven-parameter model (maxdO, minsssN, RDF55v, VE3_D, minHBint10, SpMin5_Bhs, and CrippenLogP) was also obtained with R2 and Q2 values of 0.76 and 0.70, respectively. The findings might assist in the design and development of novel CB1 modulators based on the structures of indole-2-carboxamides and N, N'-diphenyl urea

Keywords: QSAR, CB1 modulators, Indole-2-carboxamides, N,N'-diphenyl urea.

INTRODUCTION

CB1 constitutes an important target for treating drug addiction, obesity, arthritis, osteoporosis, mental illness, psychosis, and multiple sclerosis[1,2]. Several agonists/antagonists/ inverse agonists have been developed to target these G-protein-coupled receptors. Potent CB agonists like ∆9-tetrahydrocannabinol (THC) and nabilone (for treating pain) and CB1 inverse agonists such as rimonabant and taranabant (for treating obesity) were researched in a pervasive

manner in clinical settings. However, due to their extensive psychiatric side effects, anxiety-related disorders, and depression, they either were withdrawn from the market or have restricted usage[3-5]. On the contrary, CB1 allosteric modulators (compounds that bind at the allosteric sites of the CB1 receptor and alter the conformation of the primary binding site) offer an alternate and safe strategy for targeting the CB1 receptor. The allosteric modulators offer added advantages both in terms of selectivity and safety[6,7]. Cinacalcet (used in kidney disease and acts as calcium-sensing receptor agonist) and Maraviroc (anti-HIV agent and acts by CCR5 inhibition) are two examples of clinically available agents (Fig. 1) that act by allosteric modulation of their target receptors[8].

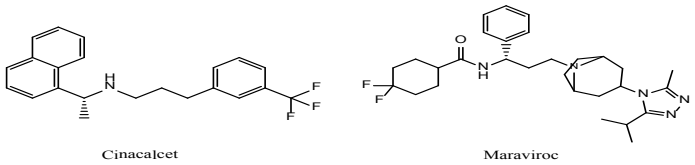

Fig. 1. Clinically available allosteric modulators

Several chemical entities like indole-based small molecules, urea-based compounds, and some tropane-bearing molecules were investigated for their potential benefits in this area (Fig. 2). It is also reported that fenofibrate and lipoxin A_4 exhibit CB1R allosteric modulator activity. In 2005, Organon Research Company identified the CB1 modulatory activity of indoles. One of the indoles, ORG27569 was considered as the prototype molecule, extensively used to elucidate the molecular mechanisms, binding site predictions and to investigate pharmacological activities. Based on this molecule several potent CB1 modulators (positive & negative) were developed. The identification of urea-based compounds as CB1 modulators started in 2007 by Prosidion Company in a high throughput screening effort. PSNCBAM-1 is considered as a lead in this chemical group of compounds and several derivatives were synthesized using this structure[10-13]. Meini and their research group tested several structural derivatives from PSNCBAM-1 for CB1 allosteric modulator activity and thoroughly discussed the SAR[14]. In recent work, Nguyen *et al.,* combined the structural features of ORG27569 and PSNCBAM-1 to design hybrid structures and screened for calcium mobilization assay. Hybrid molecules displayed similar potency as that of parent molecules. ORG27569 and PSNCBAM-1 share common pharmacophoric features and bind with the target site involved in similar types of interactions[15].

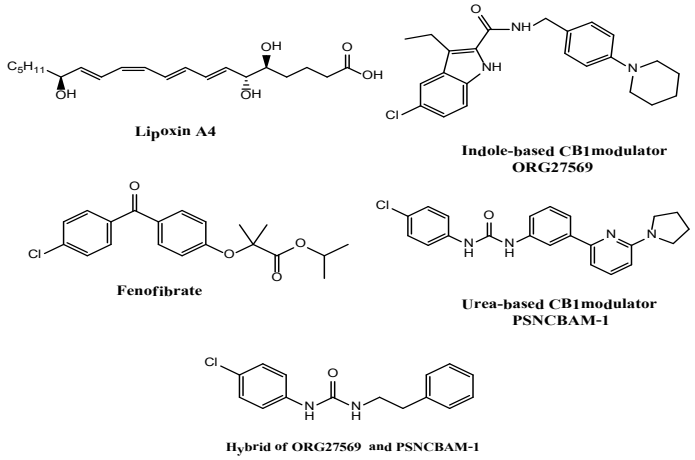

Fig. 2. Few prototype CB1 allosteric modulators

QSAR methods are gaining popularity owing to saving time, cost, and resources while simultaneously providing good hit rates[16,17]. QSAR modeling requires a thorough literature review, data collection, selection of molecular descriptors, QSAR model derivation, and finally model validation. The quality and the characteristics of the data set of compounds such as the number of compounds in the data and the activity range of the molecules significantly affect the performance of the QSAR model (predictive ability and

reliability)[18]. Molecular descriptors capture the chemical information (electronic, topological, geometrical, quantum, etc.) of a structure. Once the chemical structures are curated properly, molecular descriptors can be calculated using one or more available software tools. It is always recommended to use diverse types of molecular descriptors for better QSAR predictions[19]. To derive statistically significant QSAR models, linear and non-linear approaches are used, and the selection of the method largely depends on the dataset size and quality[18].

QSAR approaches have been proven reliable in designing CB1 receptor antagonists/ inverse antagonists. Khan *et al.,* derived robust 3D-QSAR models using a set of one hundred 1,2,4-triazole derivatives and also designed novel molecules based on the QSAR findings[20]. Similarly, using a series of 5-thiophen-2-yl pyrazoles (potent CB1 antagonists), Hanachi *et al.,* investigated the structure-activity relationship. Authors identified molecular subunit structures that can mimic rimonabant (anti-obesity agent) at the active site[21]. CB1 receptor allosteric modulators hold great therapeutic potential (anti-obesity & central analgesics) but suffer from several challenges during the preclinical and clinical studies. Given the promising insights that can be derived from QSAR modeling, it was aimed to develop QSAR models for a set of CB1 allosteric modulators including two potent classes of compounds i.e., N, N'-diphenyl urea and 1H indole-2-carboxamide derivatives. The objective is to develop QSAR models that can identify the key molecular descriptors associated with CB1 allosteric modulator activity and have high predictive ability

EXPERIMENTAL

Molecular Modeling Hardware and Software

Dataset of compounds

All the chemical structures were extracted from the literature[22-25]. The data set of compounds belongs to two structural classes (Fig. 3), one group of eighty derivatives of N, N'-diphenyl urea (Table 1: A, C, D series of compounds) and another group of thirty-four compounds, which represent the derivatives of 1H indole-2-carboxamide derivatives (Table 2: B series). The IC_{50} values (calcium mobilization assay) of the compounds (one hundred and fourteen) were then converted into the pIC_{50}.

Software tools used for the QSAR modeling

For drawing the structures and converting to 3D format, Chemdraw and Marvin Sketch (https://www.chemaxon.com) were used respectively. Using Marvin, explicit hydrogens were added to the structures and then converted to 3D and saved in MDL mol format. PaDEL software allows the calculation of a diverse set of descriptors and molecular fingerprints[26]. DTC tools [http://teqip.jdvu.ac.in/QSAR_Tools/] were installed and employed for the rest of the study including pre-treatment of data (V-WSP version 1.2 tool), model building and validation (DTC-QSAR tool version 1.0.7). For dataset division, the Kennard Stone algorithm was selected, which is a more rational data-splitting technique compared to the random division. GA-MLR (The genetic algorithm combined with multiple linear regression) technique was employed to obtain QSAR models. This technique is superior to the conventional step-wise MLR approach, as it can effectively select more relevant variables (molecular descriptors) and produce more interpretable QSAR models[27].

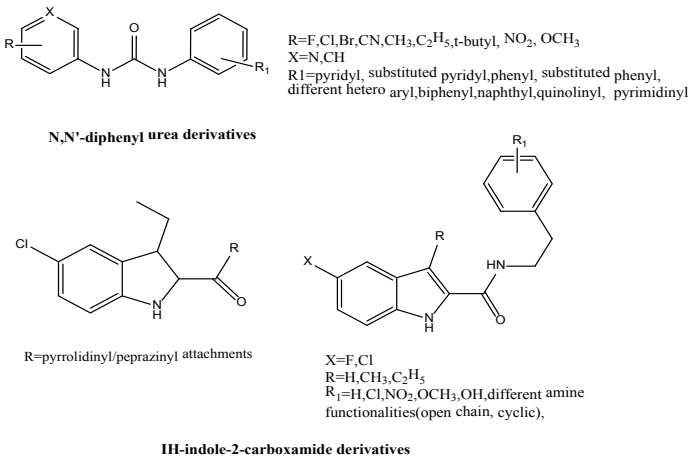

Fig. 3. General structures of compounds chosen for the QSAR study

Model Validation

QSAR models (internal & external) were evaluated for predictive power. Internal validation parameters were calculated for the training set, which include, R^2, R^2_{adj}, SEE, Q^2 (LOO), SDEP (LOO), Scaled Average R^2_m (LOO), Scaled Delta R^2_m (LOO), and MAE. The test set was used for external validation to assess the constructed model's prediction power on a new set. External validation metrices were calculated including Q^2 (F1), Q^2 (F_2), Scaled Average R^2_m, Scaled Delta R^2_m, CCC and MAE[28-30] (Tables 3 & 4).

Applicability Domain

This technique determines the presence of response outliers (a compound that exhibits activity in an unexpected manner compared to other compounds in the data set) and structural outliers in the test set and training set compounds, respectively. A standardized approach developed by Roy *et al.,* 2015 was used for this purpose[31].

Table 1: Structures, IC_{50} and pIC_{50} of compounds having N, N'-diphenyl urea nucleus

Sr. No	ID	Structure	IC_{50} (nm)	pIC_{50}
1	A1	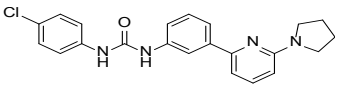	32.5	7.488
2	A2	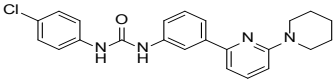	95	7.022
3	A3	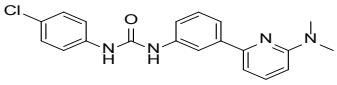	27.4	7.562
4	A4	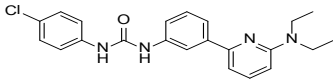	125	6.903
5	A5	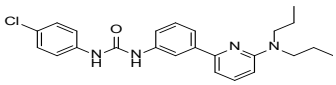	372	6.429
6	A6	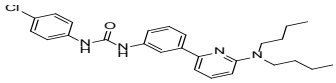	693	6.159
7	A7	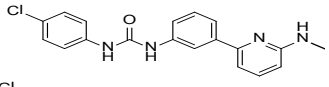	317	6.498
8	A8	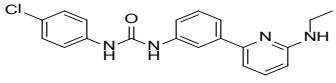	181	6.742
9	A9	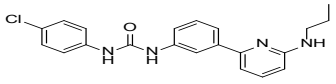	311	6.507
10	A10	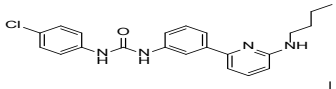	93	7.031
11	A11	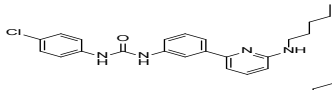	867	6.061
12	A12	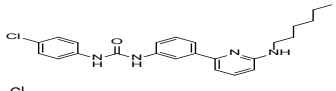	1360	5.866
13	A13	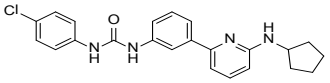	501	6.3
14	A14	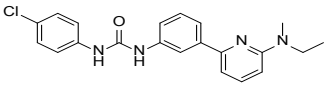	53.7	7.27

15	A15	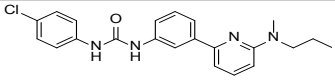	156	6.806
16	A16	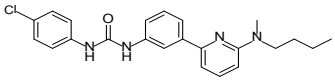	104	6.982
17	A17	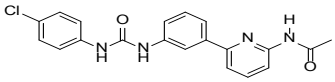	251	6.6
18	A18	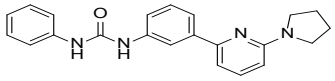	166	6.779
19	A19	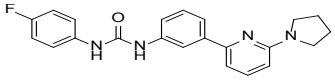	32	7.494
20	A20	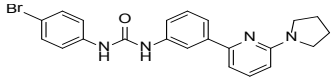	98	7.008
21	A21	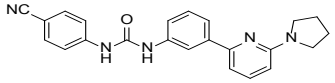	33	7.481
22	A22	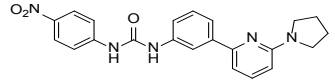	100	7
23	A23	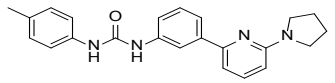	203	6.692
24	A24	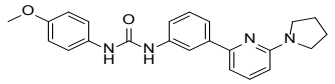	189	6.723
25	A25	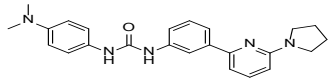	1640	5.785
26	A26	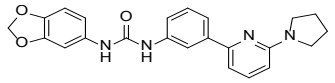	312	6.505
27	A27	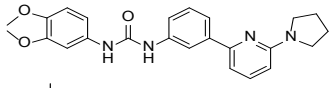	>10000	5
28	A28	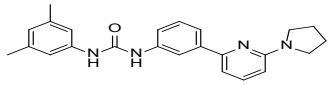	1880	5.725
29	A29	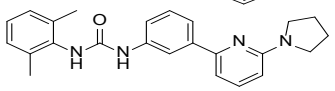	>10000	5
30	A30	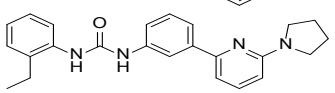	>10000	5
31	A31	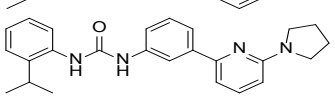	>10000	5
32	A32	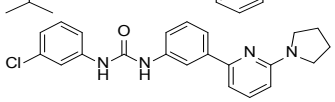	228	6.642
33	A33	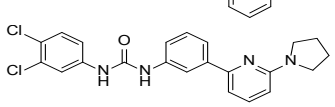	161	6.793
34	A34	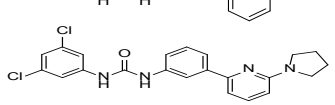	716	6.145

35	A35	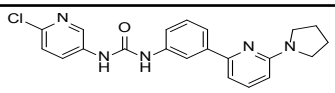	135	6.869
36	A36	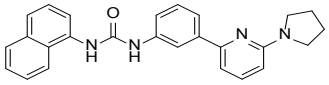	>10000	5
37	A37	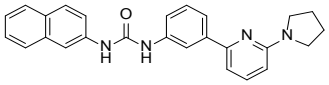	888	6.051
38	C1	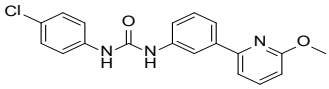	231	6.636
39	C2	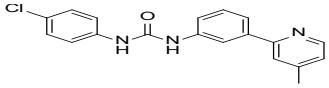	1310	5.882
40	C3	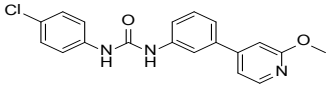	133	6.876
41	C4	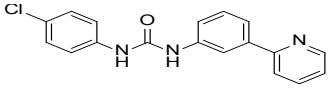	47	7.327
42	C5	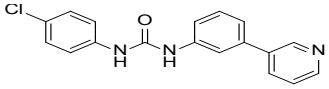	244	6.612
43	C6	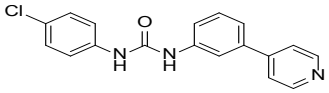	178	6.749
44	C7	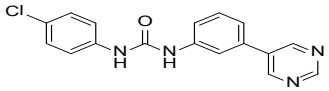	290	6.537
45	C8	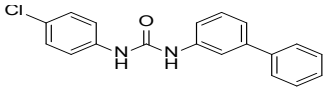	32	7.494
46	C9	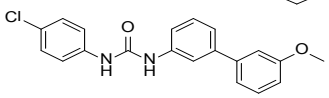	81	7.091
47	C10	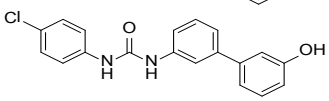	840	6.075
48	C11	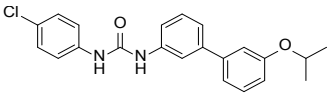	141	6.85
49	C12	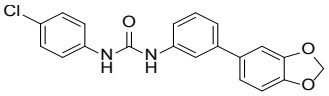	70	7.154
50	C13	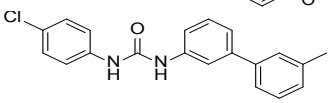	74	7.13
51	C14	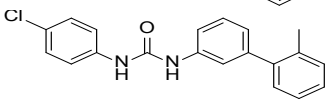	190	6.721
52	C15	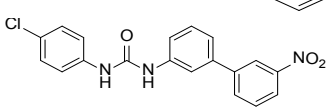	27	7.568

53	C16	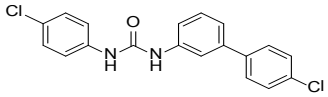	95	7.022
54	C17	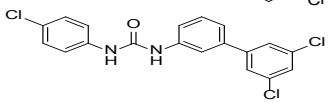	22	7.657
55	C18	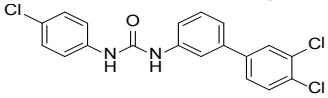	30	7.522
56	C19	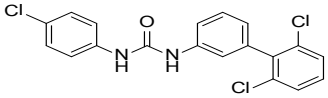	338	6.471
57	C20	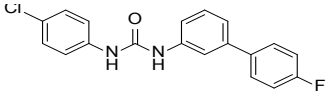	23	7.638
58	C21	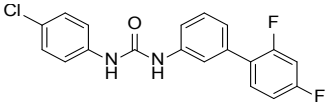	18	7.744
59	C22	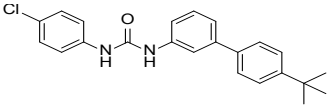	591	6.228
60	C23	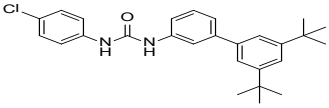	460	6.337
61	C24	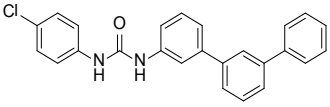	195	6.709
62	C25	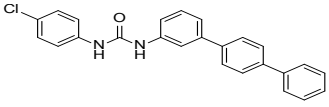	1340	5.872
63	C26	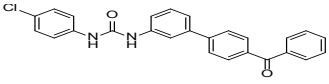	1570	5.804
64	C27	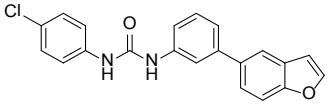	134	6.872
65	C28	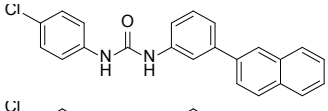	132	6.879
66	C29	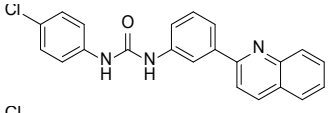	334	6.476
67	C30	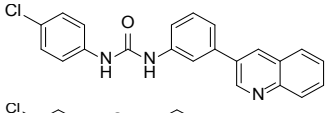	516	6.287
68	C31	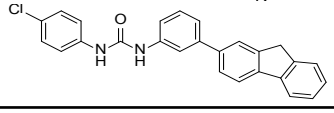	1260	5.899

69	D1	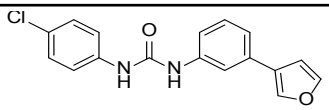	41	7.387
70	D2	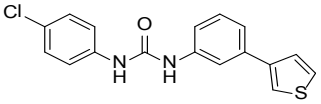	36	7.443
71	D3	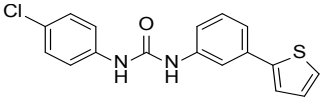	67	7.173
72	D4	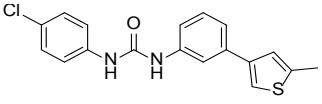	40	7.397
73	D5	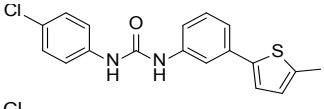	42	7.376
74	D6	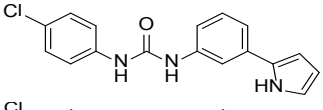	169	6.772
75	D7	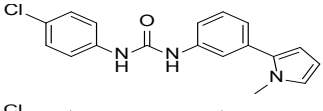	165	6.782
76	D8	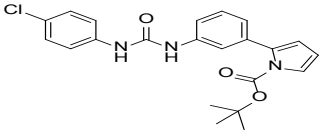	3444	5.462
77	D9	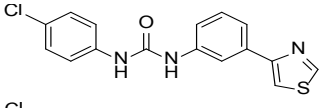	84	7.0757
78	D10	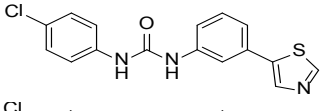	94	7.026
79	D11	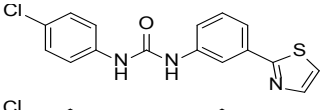	154	6.812
80	D12	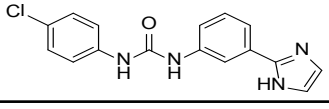	529	6.276

Table 2: Structures, IC_{50} and pIC_{50} of compounds having 1H-indole-2-carboxamide nucleus (34 compounds)

Sr. No	ID	Structure	IC_{50} (nm)	pIC_{50}
1	B1	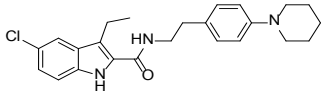	853	6.069
2	B2	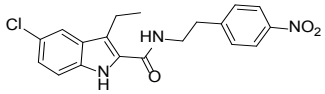	5740	5.241
3	B3	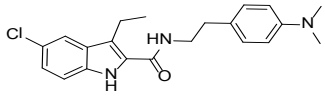	787	6.104

4	B4	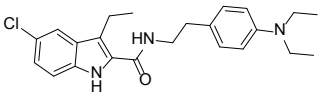	483	6.316
5	B5	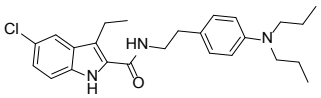	1800	5.744
6	B6	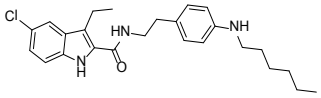	3620	5.441
7	B7	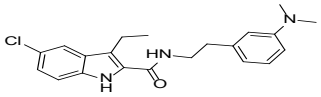	>10000	5
8	B8	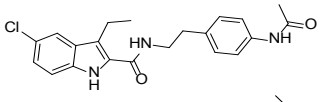	>10000	5
9	B9	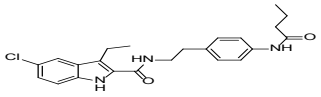	>10000	5
10	B10	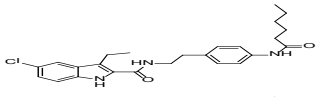	>10000	5
11	B11	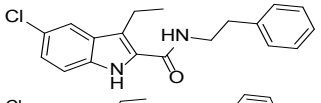	3150	5.501
12	B12	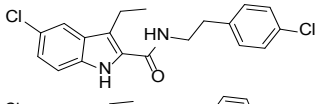	2500	5.602
13	B13	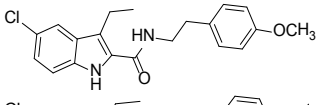	2560	5.591
14	B14	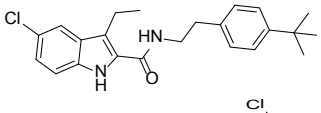	2430	5.614
15	B15	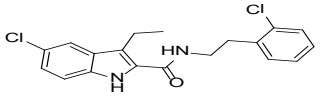	5810	5.235
16	B16	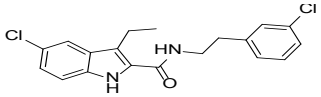	831	6.08
17	B17	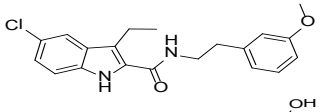	2100	5.677
18	B18	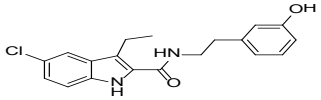	>10000	5
19	B19	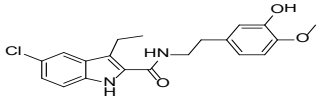	>10000	5
20	B20	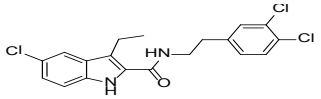	2170	5.663

21	B21	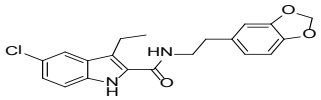	4320	5.364
22	B22	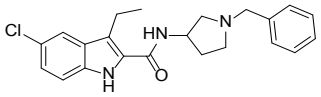	4760	5.322
23	B23	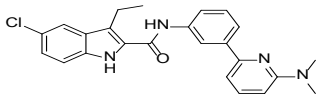	>10000	5
24	B24	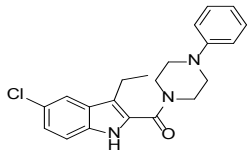	>10000	5
25	B25	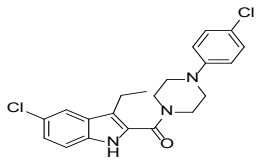	>10000	5
26	B26	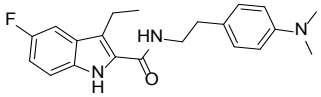	205	6.688
27	B27	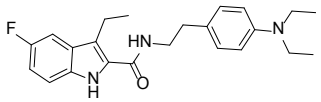	361	6.442
28	B28	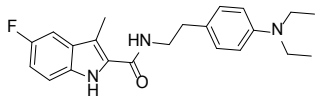	151	6.821
29	B29	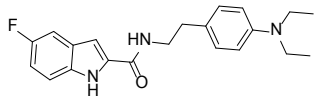	318	6.497
30	B30	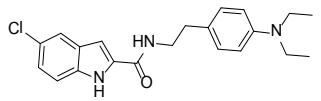	79	7.102
31	B31	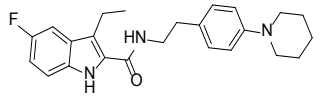	605	6.218
32	B32	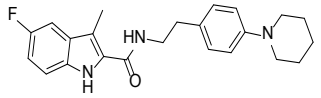	279	6.554
33	B33	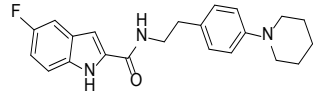	319	6.496
34	B34	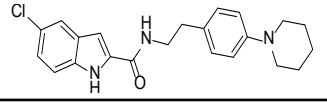	212	6.673

RESULTS AND DISCUSSION

In this study, QSAR models were derived using CB1 allosteric modulators to investigate the relationship between molecular descriptors and their potency. Chemically, the compounds

contain two different scaffolds, N, N'-diphenyl urea analogs and 1H indole-2-carboxamide derivatives. N, N'-diphenyl urea derivatives were substituted at both ring A (4^{th} position is substituted with different electron-donating and withdrawing groups) and ring B (4^{th} position is substituted with different aryl & hetero aryl groups), while 1H-indole-carboxamide derivatives were substituted on amide nitrogen directly or indirectly (ethylene linker) with various amine functionalities. Initially, all the structures were drawn and then converted to 3D formats. Then, a total of 1875 descriptors were calculated for all the compounds using the PaDEL tool. Next, using the V-WSP tool, 740 redundant descriptors were removed, based either on variance cut-off (0.0001), or correlation cut-off (0.99) in addition to the inter-correlated descriptors. Total compounds were divided into a training set (80 compounds: 70%) and a test set (34 compounds: 30%). QSAR models were developed using the GA-MLR algorithm following OECD guidelines for assessment and validation[35]. Among all the derived models, two noteworthy models were selected whose equations are described as GA-MLR model-1 and GA-MLR model-2. The models were selected based on the acceptable values of R^2(>0.6), Q^2(>0.5), Q^2F_1(>0.6), Scaled Average R^2_m LOO(>0.5), Scaled Delta R^2_m(LOO) (<0.2).

GA-MLR Model-1

MLR equation

pIC_{50} = 44.2595(+/-3.6206)-2.4957(+/-0.2572) maxdO + 0.4716(+/-0.1113) minsssN -3.6929(+/-1.9321) SpMin2_Bhm.

The model-1 built using three parameters (SPMin2_Bhm, maxdO, and minsssN) showed a good correlation with the activity. The model could explain a 65% variance in the activity of compounds (R^2: 0.65). The model fulfilled the criteria for statistical significance with R^2 = 0.65 (goodness of fit is satisfactory), Q^2 = 0.62 (good predictive ability), and $Q^2 F_1$ = 0.63 (good external predictive ability)[32-34]. Training and test sets were evaluated using internal and external validation metrics. The number of descriptors is acceptable as indicated by the minute difference (0.01) between R^2 and R^2_{adj}. The overfitting problem arises in QSAR studies due to high variance and complexity. This problem can be identified using the difference between R^2 and Q^2 (LOO). A value of 0.3 indicates over fitting problem in a QSAR model. For model-1, the value was 0.03, revealing no overfitting issues.

As per model-1, SPMin2_Bhm and maxdO are negatively contributing while minsssN is positively contributing to the activity. The descriptors, maxdO, and minsssN represent electro-topological state atom (E-state) type descriptors whereas SPMin2_Bhm, descriptor explains the mass of the compounds[26]. The e-state of any atom is a sum of 1) the contribution of the intrinsic and topological status of that atom (I_i) and 2) the effect of the environment (ΔI_i). E-state value increases when electronegativity/electro density increases and the value decreases with branching in the molecule[32]. According to the equation, the high electronegativity of the doubly bonded oxygen, maxdO (carbonyl oxygen) is detrimental to the activity. Reducing the electron density of oxygen atoms might have a positive influence on the activity. It can be observed that substituted 1H-indole 2- 2-carboxamides (B1-B34), where high electronegativity on carbonyl oxygen is high, are comparatively less potent compared to substituted N, N'-diaryl urea analogs.

Minsss N (an atom-level topological index) is positively contributing to the activity. With this descriptor, it is possible to explain the potent activity of the dataset of compounds possessing substituted amine group (A1-A6, A14-A16, A18-A37) in comparison to compounds containing secondary amine group (A7-A13, A17, B6, B8-B10). E-states of atoms describe electrostatic potential, which is a suitable feature to analyze non-covalent interactions (suitable for protein-ligand interactions). SPMin2_Bhm is negatively contributing to the activity, indicating bulkiness as an unfavorable feature. The low activity of indole carboxamides (B2, B3, B5, B9, B14, B23, B27, B28, B31, B32) and urea derivatives possessing bulkier groups on phenyl rings (A28-A31, A36, A37, C28, C29, C31 C24, C25, C26) can be well correlated with their with high SPMin2_Bhm values.

GA-MLR Model-2

MLR equation

pIC_{50} = 39.1907(+/-2.9279) -0.0527(+/-0.0195) RDF55v-2.6088 (+/-0.2551) maxdO + 0.0858 (+/-0.0299) VE3_D + 0.1064 (+/-0.0463) minHBint10 -1.074 (+/-0.463) SpMin5_Bhs + 0.387 (+/-0.059) minsssN + 0.2582 (+/-0.0616) Crippen LogP

The model showed a high ability to explain the variance (76%) in the CB1 modulator activity. The improved model met the requirements for robustness, internal and external prediction ability with R^2 = 0.76, Q^2 = 0.70, and Q^2 F_1 = 0.715. Scaled Average R^2_m LOO, Scaled Delta R^2_m LOO, and CCC values were found to be 0.599, 0.16, and 0.79, better than model-1 (0.495, 0.236, and 0.69) indicating better model predictivity and accuracy.In model 2, maxdO, minsssN, RDF55v, VE3_D, minHBint10, SpMin5_Bhs, and Crippen LogP showed a good correlation with the activity of the compounds. The negative contribution of maxdO, SPMin2_BHs (topological distance matrix describes relative I-state), and RDF55v is indicated in this model. RDF (radial distribution function) related descriptors are based on the distance distribution in the geometrical representation of a molecule. RDF55v, the van der Waals volume distribution in three dimensions, is computed at a radius of 5.5 A using the unique geometric centers of each molecule. This descriptor highlights the crucial role of a molecular conformation and the role of van der Waals volume for activity at CB1 receptor[33]. The contribution of RDF55 revealed a higher possibility of interaction with the hydrophobic pocket of the receptor.

We could correlate the influence of this descriptor with conformational possibilities of N, N'-diaryl urea analogs. N, N'-diaryl urea analogs have unique conformational preferences and exhibit more dynamic behavior. It depends on the substitution whether the molecule prefers to be in either cis or trans-conformation. If the nitrogen atoms are unsubstituted, cis conformation is preferred for the molecule. Urea derivatives in the data set possess unsubstituted nitrogen atoms, suggesting a possible cis conformation for the molecules. The cis geometry of the urea derivatives might be a contributing factor for high potency compared to the indole carboxamides[34]. VE3_D is a 2D-matrix-based index. Higher values of VE3_D (less branching in a molecular structure) are favourable for the activity. This descriptor encodes the electronic, topological, and geometrical features of the compounds. Crippen Log P denotes the atomic contribution of log P and minHBint10 which is a 2D autocorrelation descriptor that denotes the count of E-state descriptors of strength for potential hydrogen bonds of path length 10. The dependence of activity on these descriptors indicates that atomic mass and electronic distribution are controlling the activity. In the present QSAR analysis, we were able to identify the difference in potency of diphenyl urea derivatives and indole carboxamides towards CB1 is majorly due to the differences in the geometry of the molecules and due to variation in the electron density on the carbonyl oxygen.

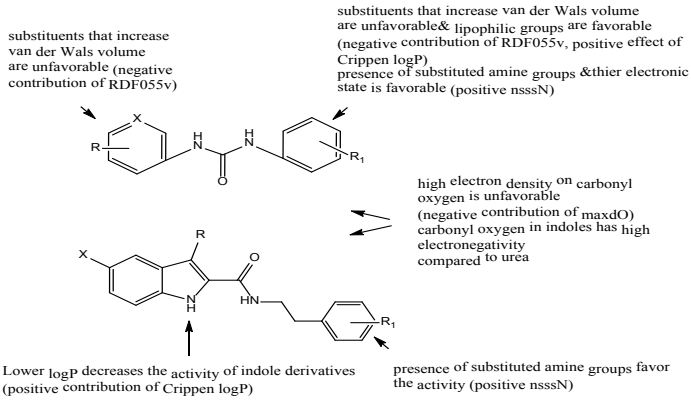

Fig. 4. Contributions from various descriptors

Table 3: Internal and External Validation Parameters (GA-MLR Model-1)

Parameter in Training Set	Value	Parameter in Test Set	Value
R^2	0.65	Q^2 (F_1) Test	0.63
R^2_{adj}	0.64	Q^2 (F_2) Test	0.48
Standard Estimation of Error (SEE)	0.45	Scaled Average R^2_m (Test)	0.35
Q^2 (LOO)	0.62	Scaled Delta R^2_m (Test)	0.30
SDEP (LOO)	0.46	CCC (Test)	0.69
Scaled Average R^2_m (LOO)	0.49	MAE, Test)	0.42
Scaled Delta R^2_m (LOO)	0.23		
Mean Absolute Error (MAE, Model Predicted)	0.35		
MAE, LOO)	0.37		

Table 4: Internal and External Validation Parameters (GA -MLR Model-2)

Parameter in Training Set	Value	Parameter in Test Set	Value
R^2	0.76	Q^2 (F_1) Test	0.71
R^2_{adj}	0.73	Q^2 (F_2) Test	0.60
SEE	0.39	Scaled Average R^2_m (Test)	0.55
Q^2 (LOO)	0.70	Scaled Delta R^2_m (Test)	0.22
SDEP (LOO)	0.41	CCC (Test)	0.79
Scaled Average R^2_m (LOO)	0.59	MAE, Test	0.38
Scaled Delta R^2_m (LOO)	0.16		
MAE, Model Predicted	0.27		
MAE (LOO)	0.30		

The influence of various molecular descriptors was depicted in Fig. 4. The statistical significance of the derived QSAR models was validated using standard parameters, well recognized in the QSAR field[35-37]. However, the quality of QSAR models heavily depends on the quality of input data, similar to that of machine learning models. Currently, our data is limited to only two chemical classes of compounds. In the future, we will further improve the models by re-training the models with additional data.

CONCLUSION

N, N'-diphenyl urea and 1H-indole-2-carboxamide derivatives can modulate the actions of CB1 receptors effectively. Though the atomic composition and molecular connectivity are different, these two classes of compounds exhibit promising CB1 receptor modulation. In the present QSAR investigations, two statistically significant models were derived from a set of 114 CB1 modulators. Among all the obtained descriptors, we observed the prominent contribution of maxdO and RDF55v toward the activity. The receptor binding ability of N, N'-diphenyl urea, and 1H-indole-2-carboxamide derivatives might be inversely correlated with RDF55v (geometry) and maxdO (charge on the carbonyl oxygen). The present QSAR findings might contribute to design and finetune the CB1 allosteric modulators.

ACKNOWLEDGMENT

The authors acknowledge the constant help and guidance rendered by Dr. Pravin Ambure in compiling the manuscript.

Conflict of interest

The author declare that we have no conflict of interest.

REFERENCES

1. Mackie, K., *Annu. Rev. Pharmacol. Toxicol.*, **2006**, *46*(1), 101-122.
2. Cinar, R.; Iyer, M. R.; Kunos, G., *Pharmacol. Ther.*, **2020**, *208*, 107477.
3. Haller., *J. Int. J. Mol. Sci.*, **2023**, *24*, 15777.
4. Bosquez-Berger, T.; Szanda, G.; Straiker, A., *Drugs Drug Candidates.*, **2023**, *2*, 689-707.
5. Murphy, T.; Le Foll, B., *Biomolecules.*, **2020**, *10*, 855.
6. Khurana, L.; MackiE. K.; Piomelli, D.; Kendall, D, A., *Neuropharmacology.*, **2017**, *124*, 3-12.
7. Kulkarni, A. R.; Garai, S.; Janero, D. R.; Thakur, G. A., *Methods. Enzymol.*, **2017**, *593*, 281-315.

8. Ahn, S.; Pani, B.; Kahsai, A. W.; Olsen, E. K.; Husemoen, G.; Vestergaard, M.; Jin, L.; Zhao, S.; Wingler, L. M.; Rambarat, P. K.; Simhal, R. K.; Xu, T. T.; Sun, L.D.; Shim, P.J.; Staus, D. P.; Huang, L.; Franch, T.; Chen, X.; Lefkowitz, R., *J. Mol. Pharmacol.*, **2018**, *94*(2), 850-861.
9. Changeux, J. P.; Christopoulos, A., *Cell.*, **2016**, *166*(5), 1084-1102.
10. Nguyen, T.; Li, J.; Thomas, B. F.; Wiley, J. L, Kenakin, T. P.; Zhang, Y., *Med. Res. Rev.*. **2017**, *37*(3), 441-474.
11. Dopart, R.; Lu, D.; Lichtman, A. H.; Kendall, D. A., *Drug. Metab. Rev.*, **2018**, *50*(1), 3-13.
12. Lu, S.; Zhang, J. S., *J. Med. Chem.*, **2019**, *62*(1), 24-45.
13. Morales, P.; Goya, P.; Jagerovic, N.; Hernandez-Folgado, L. Cannabis., *Cannabinoid Res.*, **2016**, *1*(1), 22-30.
14. Meini, S.; Gado, F.; Stevenson, L. A.; Digiacomo, M.; Saba, A.; Codini, S.; Macchia, M.; Pertwee, R. G.; Bertini, S.; Manera, C.; Manera, C., *Eur. J. Med. Chem.*, **2020**, *203*, 112606.
15. Nguyen, T.; Thomas, B. F.; Zhang, Y., *Current Topics in Medicinal Chemistry.*, **2019**, *19*(16), 1418-1435.
16. Maltarollo, V. G.; Kronenberger, T.; Wrenger, C.; Honorio, K. M., *C Future. Sci.*, OA., **2017**, *3*(4). FSO214.
17. Neves, B. J.; Braga, R. C.; Melo-Filho, C. C.; Moreira-Filho, J. T.; Muratov, E. N.; Andrade, C. H., *Front. in Pharmacol.*, **2018**, *9*, 1275.
18. Roy, K.; Kar, S.; Das, R.N. QSAR/QSPR Modeling: Introduction. In: A Primer on QSAR/QSPR Modeling. SpringerBriefs in Molecular Science. Springer, Cham., **2015.**
19. Grisoni, F.; Ballabio, D.; Todeschini, R.; Consonni, V., *Methods Mol Biol.*, **2018**, *1800*, 3-53.
20. Khan, N.; Halim, S. A.; Khan, W.; Zafar, S. K.; Ul-Haq, Z., *Journal of Molecular Graphics and Modelling.*, **2019**, *89*, 199-214.
21. Hanachi, R..; Said, R. B.; Allal, H.; Rahali, S.; Alkhalifah, M. A.; Alresheedi, F.; Tangour, B.; Hochlaf, M., *New J Chem.*, **2021**, *45*(38), 17796-17807.
22. Nguyen, T.; German, N.; Decker, A. M.; Li, J. X.; Wiley, J. L.; Thomas, B. F.; Kenakin, T. P.; Zhang, Y., *Bioorg Med Chem.*, **2015**, *23*(9), 2195-2203.
23. Nguyen, T.; Gamage, T. F.; Decker, A. M, German, N.; Langston, T. L.; Farquhar, C.E.; Kenakin, T. P.; Wiley, J.L.; Thomas, B. F.; Zhang, Y., *ACS Chem. Neurosci.*, **2019**, *10*(1), 518-527.
24. German, N.; Decker, A. M.; Gilmour, B. P.; Gay, E. A.; Wiley, J. L.; Thomas, B. F.; Zhang, Y., *J. Med. Chem.*, **2014**, *57*(18), 7758-7769.
25. Nguyen, T.; German, N.; Decker A. M.; Langston, T. L.; Gamage, T. F.; Farquhar, C.E.; Li, J. X.; Wiley, J. L.; Thomas, B. F.; Zhang, Y., *J. Med. Chem.*, **2017**, *60*(17), 7410-7424.
26. Yap, C. W. P., *J. Comput. Chem.*, **2011**, *32*(7), 1466-1474.
27. Kennard, R. W.; Stone, L, A., *Technometrics.*, **1969**, *11*(1), 137-148.
28. Ambure, P.; Gajewicz-Skretna, A.; Cordeiro, M. N. D. S.; Roy, K., *J. Chem. Inform. Model.*, **2019**, *59*(10), 4070-4076.
29. Tropsha, A., *Mol. Inf.*, **2010**, *29*(6-7), 476-488.
30. Veerasamy, R.; Rajak, H.; Jain, A.; Sivadasan, S.; Christapher, P. V.; Agrawal, R., *Int J Drug Design and Discov.*, **2011**, *2*, 511-519.
31. Roy, K.; Kar, S..; Ambure, P., *Chemometrics and Intelligent Laboratory Systems.*, **2015**, *145*, 22-29.
32. Hall, L. H.; Kier, L. B., *J. Chem. Inf. Comput. Sci.*, **1995**, *35*(6), 1039-1045.
33. Hemmer, M. C.; Gasteiger., *J. Analytica Chimica Acta.*, **2000**, *420*(2), 145-154.
34. Bryantsev, V. S.; Firman, T. K.; Hay, B. P., *The Journal of Physical Chemistry A.*, **2005**, *109*(5), 832-842.
35. Golbraikh, A.; Tropsha, A., *J. Comput Aided Mol Des.*, **2002**, *16*(5/6), 357-369.
36. Gramatica, P., *Methods Mol. Biol.*, **2013**, *930*, 499-526.
37. Roy, K.; Chakraborty, P.; Mitra, I.; Ojha, P.K.; Kar, S.; Das, R. N., *J Comput Chem.*, **2013**, *34*(12), 1071-1082.